

Design and Simulation of All Optical Photonic Crystal Wavelength Selective Devices Based on Directional Couplers for Optical Communication Systems

Saeed Ghorbani*, Reza Mosalanezhad, Gholam Reza Ghadar

Department of Electronics Engineering, Fasa Branch, Islamic Azad University, Fasa, Iran

Received: 13 October 2017

Accepted: 09 November 2017

Published: 01 December 2017

Abstract

In this paper, the all optical wavelength selective devices based on directional couplers are provided using in new geometrical structures from 2D photonic crystal in the form of dielectric rods all arranged in a square lattice. Plane wave expansion and finite difference time domain methods have been utilized in TM polarization mode at CFS-PML boundary condition as the absorber area surrounding the calculational area in order to calculate the results and also simulate the proposed devices in this paper. In this paper we have tried to change the location of the bending in the length of presented structures by increasing the amplitude of the transmitted signal. The optical input signal lead to the output port by choosing a proper length for coupling region and desired frequency with maximum amplitude.

Keywords: Photonic Crystal; Optical Directional Coupler; Finite-Difference-Time-Domain (FDTD); Plane Wave Expansion (PWE); Photonic Band Gap

How to cite the article:

S. Ghorbani, R. Mosalanezhad, G. R. Ghadar, Design and Simulation of All Optical Photonic Crystal Wavelength Selective Devices Based on Directional Couplers for Optical Communication Systems, Medbiotech J. 2017; 1(4): 182-187, DOI: 10.22034/mbt.2017.87082

1. Introduction

Photonic crystals (PhCs) are novel class of optical media represented by natural or artificial structures with periodic modulation of the refractive index. During the last years, much attention has been paid to photonic crystals. In a photonic crystals, some gaps can be produced in band structure that electromagnetic waves can't transport in some distinct frequencies [1,2]. Photonic crystals are so considerable for their control capabilities and electromagnetic wave guidance. With the successful demonstration of the photonic band gap [3], focus turned to the engineering of devices utilizing the photonic band structure. Various types of optoelectronic devices, such as channel-drop filters [4,5] (Djavid et al., 2008; Djavid et al., 2008), Mach-Zehnder interferometers [7], power splitters [8-10] and

other devices based on PhCs, have been investigated. These devices usually have many advantages, such as substantial size reduction, compared with their conventional counterparts [3,10]. In this paper, we focus on optical wavelength selective devices based on directional couplers. All optical wavelength selective devices based on directional couplers have been studying in recent years due to their potential abilities for using them in optical system. The couplers execute a variety of functions in conventional optical devices, including power splitting [6,11-12].

In this paper, two new geometrical structures of 2D photonic crystals arranged in a square lattice have been used to design and simulation of all optical wavelength selective devices based directional coupler. Several numerical methods have been employed for analysis of the optical devices based on photonic crystals. Current research has used

* Corresponding Author Email: s.ghorbani2010@gmail.com

PWE method to calculate diagram of the band structure and characterize the photonic band gap [13], while using FDTD numerical method with CFS-PML boundary condition to show field emission in structure of these devices.

2. Methodology

2.1 Plane Wave Expansion Method

Designing the PhC-based optical devices for applications in band gap, first needs to specify the photonic band gap using the diagram of photonic band structure. Plane wave expansion (PWE) method was applied to calculate this diagram. The starting point of PWE method is from Maxwell's equations. In this paper, diagrams of optical band structure of photonic crystals, using plane wave expansion method, is studied for the first eight bands and in TM modes. Equation 1 is expressed the final eigenvalue equations for magnetic fields in plane wave expansion method. For magnetic field, the equation is shown as:

$$\sum_G \kappa(G - G') \kappa(k + G') A(k + G) = \frac{\omega^2}{c^2} A(k + G) \quad (1)$$

Where G is the reciprocal lattice vector, κ is the fourier coefficient, k is the wave vector, C and A are coefficients.

2.2 Two-Dimensional FDTD Method

We have employed 2D FDTD based on the well-known Yee algorithm [14], which does not have such limitations. The starting point of FDTD method, like PWE, method is from Maxwell's equations as follows:

$$\frac{1}{\mu} \nabla \times \vec{E}(r, t) = -\frac{\partial \vec{H}(r, t)}{\partial t} \quad (2)$$

$$\frac{1}{\varepsilon} \nabla \times \vec{H} = \frac{\partial \vec{E}(r, t)}{\partial t} \quad (3)$$

Where μ and ε are the permeability and permittivity, respectively. The electromagnetic fields are calculated by solving Maxwell's equations in a finite difference scheme in the time domain. After discretization of Maxwell's equations (equations 2 and 3) the following set of discretized equations is obtained. The 2D FDTD time stepping formulas for the TM modes are:

$$E_{z(i,j)}^{n+1} + \frac{\Delta t}{\varepsilon} \left(\frac{H_{y(i+\frac{1}{2},j)}^n - H_{y(i-\frac{1}{2},j)}^n}{\Delta x} \right) - \left(\frac{H_{x(i,j+\frac{1}{2})}^n - H_{x(i,j-\frac{1}{2})}^n}{\Delta y} \right) \quad (4)$$

$$H_{y(i+\frac{1}{2},j)}^{n+1} = H_{y(i+\frac{1}{2},j)}^{nn} + \frac{\Delta t}{\mu} \left(\frac{E_{z(i+1,j)}^{n+\frac{1}{2}} - E_{z(i,j)}^{n+\frac{1}{2}}}{\Delta x} \right) - \left(\frac{E_{x(i+\frac{1}{2},j+1)}^{n+\frac{1}{2}} - E_{x(i+\frac{1}{2},j-1)}^{n+\frac{1}{2}}}{\Delta y} \right) \quad (5)$$

$$H_{x(i,j+\frac{1}{2})}^{n+1} = H_{x(i,j+\frac{1}{2})}^{nn} + \frac{\Delta t}{\mu} \left(\frac{E_{z(i,j+\frac{1}{2})}^{n+\frac{1}{2}} - E_{z(i,j-\frac{1}{2})}^{n+\frac{1}{2}}}{\Delta z} \right) - \left(\frac{E_{y(i,j+1)}^{n+\frac{1}{2}} - E_{y(i,j-1)}^{n+\frac{1}{2}}}{\Delta y} \right) \quad (6)$$

where, the n denotes the discrete time step, indices i and j denote the discretized grid point in the x - y planes, respectively. The sampling in time is selected to ensure numerical stability of the algorithm, by

$$\Delta t \leq \frac{1}{c} \frac{1}{\sqrt{\frac{1}{(\Delta x)^2} + \frac{1}{(\Delta y)^2}}} \quad (7)$$

Where C is the speed of light.

All programs (PWE and FDTD) in this paper use the MATLAB programming language running on Laptop with CPU powers of 2.3 GHz and Intel core i5 processors and 4 GB of memory.

2.3 Directional Coupler and the Coupling Mechanism

A directional coupler can be obtained by removing two rows of rods adjacent to a central row. When two PC waveguides are placed close to each other, light propagating in one of the waveguides can be coupled to the neighboring waveguide after passing a certain distance referred to as the coupling length. The coupling length L_c is the distance over which the phase difference between two modes is 180° , which depends on the difference between propagation constants of the odd and even modes. The coupling length can be described as follow:

$$L_c = \frac{\Pi}{|\beta_{even} - \beta_{odd}|} \quad (8)$$

2.4 Design and Simulation

Figure. 1 shows the initial photonic crystal structures consisting of silicon rods with refractive index $n = 3.4$ in the air ($n = 1$) arranged by a square lattice, with lattice constant ($a = 0.483 \text{ m}$).

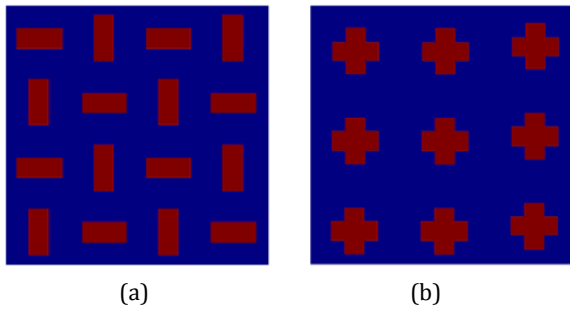


Figure 1. Two-dimensional photonic crystals with Honeycomb lattice.

As is seen, we can design photonic crystals in new shapes. Photonic crystals in this paper are all in square lattice structure. Figure 2, shows the photonic crystal cells and Table 1 shows side length of photonic crystal in a square photonic crystal cells which shown in figure 2.

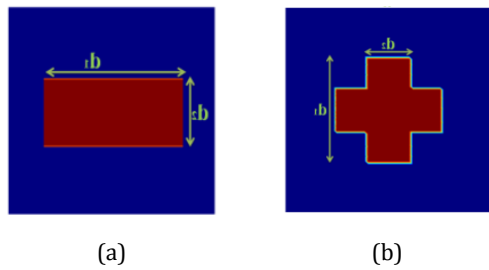


Figure 2. Photonic crystal cells.

Table 1. The side length of photonic crystals with different shapes in a square cell.

The side length of photonic crystal		Figure
$d_1 = 0.7 a$	$d_2 = 0.3 a$	a
$d_1 = 0.5 a$	$d_2 = 0.2 a$	b

Figure 3 depicts photonic band structure diagram of the 2D photonic crystals for the first eight bands of these structures which are calculated via PWE method for TM mode. It can be seen that the presented diagram has several photonic band gap with adequate width for its first eight bands. In order to select an appropriate frequency, range for designing photonic crystal wavelength selective based on directional couplers, in this paper, the first photonic band gap of each PhC has been considered. The structure, in figure 3.a has a large band gap for TM waves in the range of $0.3044 \leq a / \lambda \leq 0.3874$ and also the structure, in figure 3.b has a large band gap for TM waves in the range of $0.272 \leq a / \lambda \leq 0.3905$. The devices design are shown in figure 4.a and figure 5.b. Each structure consists of two input W1 PhC channel waveguides connected to two outputs W1 PhC channel waveguides through a coupling region. The coupling region consists of two PhC channel waveguides placed next to each other and separated by two rows of coupling rods. The coupling length is very important in selecting the proper wavelength that come from each input ports. In this paper, every coupled region length is equal to $17a$.

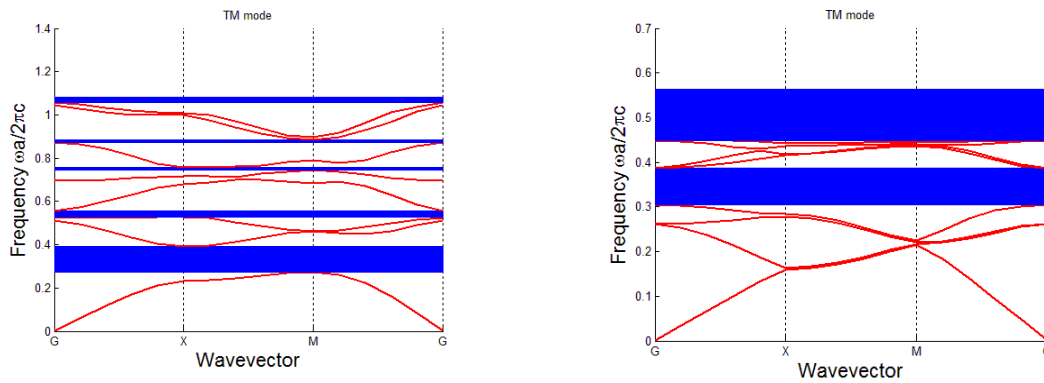


Figure 3. Photonic band structure of two-dimensional periodic photonic crystal in TM mode.

The 90° bend with the structure of figure 5.a and figure 6.b are used to connect the input to the coupling region. According to figure 5.a and figure 6.b some changes were made at the bending regions, These changes will increase the transmission of optical signals during simulation. The 2D-FDTD method has been used for simulation of each structures. We set the resolution to 21 in the FDTD simulations ($a/21$). All simulations are carried out at the same resolution in order to obtain

consistent comparison results. The Gaussian-wave source is used to excite the input waveguide in TM polarization and run for several iterations. The simulation area is surrounded by one-spatial unit thick complex frequency, shifted (CFS) PML, which absorbed the fields leaving the simulated region in order to prevent reflections. The propagation is along the z direction. The space steps in the x and z directions are Δx and Δz . Δx and Δz are selected 0.05. The sampling in time is $\Delta t=0.95$.

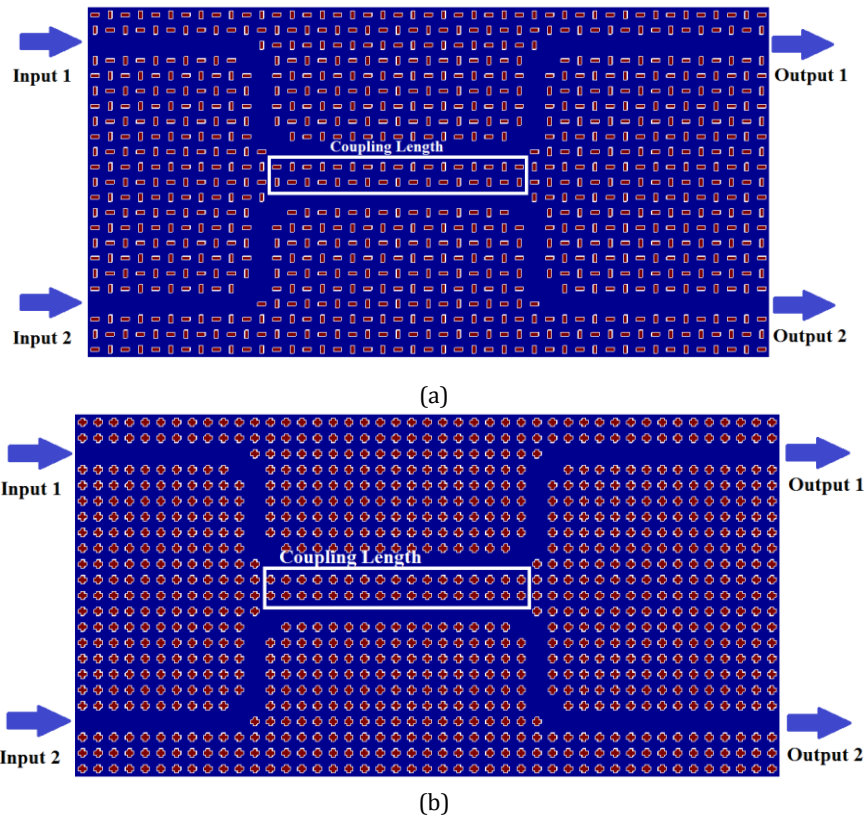


Figure 4. The proposed structures of optical photonic crystals wavelength selective devices based on directional couplers with two new geometric forms.



Figure 5. The 90° bend of the proposed structures.

A Gaussian pulse is applied to the input of each ports to determine the appropriate frequency for each of the inputs, then the electric and magnetic fields are computed at each output. With the FFT (Fast Fourier Transform) of the electric and magnetic fields and by using pointing vector integral, proper frequencies can be calculated for each input ports. In this paper, according to the band structure diagram (Figure 3) and First optical band gap calculated by PWE numerical solution method for both structured, we apply a Gaussian signal with 0.35 frequency to input 2 in the presented structures in figure 4.a and figure 4.b Maximum normalized frequencies calculated for

figure 4, a structure is equal to 0.3115 and 0.3364. FDTD numerical solution method is used to see optical signal propagation in the presented structure for obtained frequencies. Figure 5.a and Figure 5.b indicate electric field propagation in the structure presented in this paper for the normalized frequency of 0.3115 and 0.3364. By selecting normalized frequencies $f = 0.3115$ ($\lambda = 1.550\mu\text{m}$) and $f = 0.3364$ ($\lambda = 1.435\mu\text{m}$), according to Fig 6. a and Figure 6, b, the coupled optical signal occurs at the different distances from the waveguide paths and optical signal transmits to the output 1 and 2.

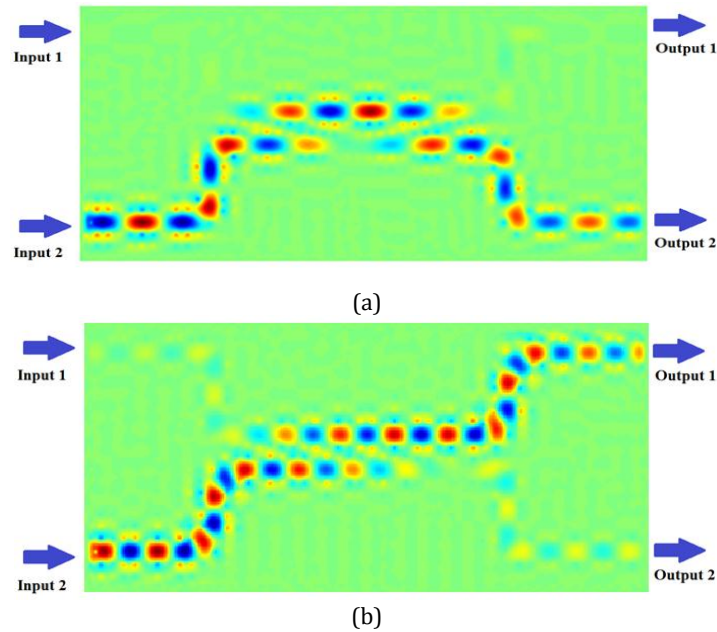


Figure 6. Electric field distributions of the directional coupler with square lattice of rods for normalized frequency of (a) $f = 0.3115$ and (b) $f = 0.3364$.

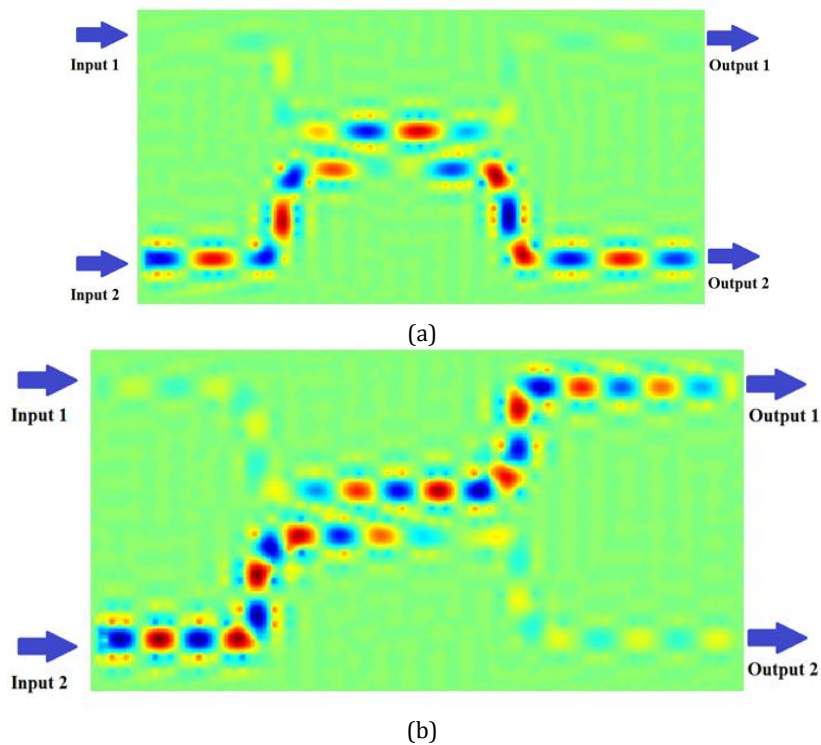


Figure 7. Electric field distributions of the directional coupler with square lattice of rods for normalized frequency of (a) $f = 0.3$ and (b) $f = 0.32$.

With this method, an optical signal with a certain frequency passes from each output ports. Similarly, for Figure 4.b structure, the maximum normalized frequency is equal to $f = 0.3$ ($\lambda = 1.61\mu\text{m}$) and $f = 0.32$ ($\lambda = 1.509\mu\text{m}$). For these two frequencies the coupled optical signal occurs at certain distances. Figure 7.a and Figure 7.b show how to propagate optical signal at frequencies 0.3 and 0.32.

3. Conclusion

In this paper, two new structures of photonic crystals have been developed with different geometries. The diagram proposed for band structure of the photonic crystals in this paper, have a sufficiently wide photonic band gap which enables designing a wide variety of the optical

devices in this frequency range. So, all optical photonic crystals wavelength selective devices based on directional couplers with these two new geometric forms have been proposed and simulated with the numerical methods. For increasing the transmission in bends region, we changed the structures of the bends region.

References

1. Zhu, N., J. Wang, C. Cheng, X. Yan. 2012. Research of band gap properties based on two-dimensional photonic crystal with mixed shapes of rods. *Optik Int. J. Light Electron Opt.* (In Press)
2. Liu, D., Y. Gao, D. Gao, X. Han. 2012. Photonic band gaps in two-dimensional photonic crystals of core-shell-type dielectric nanorod heterostructures. *Optics Communication*. 285: 1988-1992.
3. Yablonovitch, E. 1987. Inhibited spontaneous emission in solid-state physics and electronics. *Phys. Rev. Lett.* 58: 2059-2062.
4. Djavid, M., A. Ghaffari, F. Monifi, M. S. Abrishamian. 2008. Heterostructure photonic crystal channel drop filters using mirror cavities. *J. Opt. A: Pure Appl. Opt.* 10 055203 doi:10.1088/1464-4258/10/5/055203.
5. Djavid, M., A. Ghaffari, F. Monifi, M. S. Abrishamian. 2008. Photonic crystal power dividers using L-shaped bend based on ring resonators. *J. Opt. Soc. Am. B.* 25(8): 1231-1235.
6. Djavid, M., A. Ghaffari, F. Monifi, M. S. Abrishamian. 2008. T-shaped channel-drop filters using photonic crystal ring resonators. *Physica E.* 40(10): 3151-3154.
7. Martinez, A., P. Sanchis, J. Marti. 2005. Mach-Zehnder interferometers in photonic crystals. *Opt. Quantum Electron* 33: 77-93.
8. Ghaffari, A., F. Monifi, M. Djavid, M. S. Abrishamian. 2008. Analysis of photonic crystal power splitters with different configurations. *J. Appl. Sci.* 8: 1416-1425.
9. Bayindir, M., B. Temelkuran, E. Ozbay. 2000. Photonic-crystal-based beam splitters. *Appl. Phys. Lett.* 77: 3902-3904.
10. Yu, T. B., M. H. Wang, X. Q. Jiang, Q. H. Liao, J. Y. Yang. 2007. Ultra compact and wideband power splitter based on triple photonic crystal waveguides directional coupler, *J. Opt. A: Pure Appl. Opt.* 9: 37-42.
11. Wang, Y. 1999. Nonlinear optical limiter and digital optical switch by cascaded nonlinear couplers: Analysis. *IEEE J. Lightwave Technol.* 17(2): 292-297.
12. Ferreras, A., F. Rodriguez, E. Gomez-Salas, J. L. de Miguel, F. Hernandez-Gil. 1993. Useful formulas for multimode interference power splitter/combiner design, *IEEE Photon. Technol. Lett.* 5(10): 1224-1227.
13. Zhang, H. T., D. S. Wang, M. L. Gong, D. Z. Zhao. 2004. Application of group theory to plane wave expansion method for photonic crystals. *Optics Communication* 237: 179-187.
14. Yee, K. S. 1966. Numerical solutions of initial boundary value problems involving Maxwell's equation in isotropic media. *IEEE Trans, on Antennas and Propagation* 14(3): 302-307.